25. Black DM, Cummings SR, Melton JL III. Appendicular bone mineral and a women's lifetime risk of hip fracture. J Bone Miner Res 1992;7:639–646.
26. Lauritzen JB, Schwarz P, Lund B, McNair P, Transbol I. Changing incidence and residual lifetime risk of common osteoporosis-related fractures. Osteoporosis Int 1993;3:127–132.
27. Arenberg D. Misclassification of "probable senile dementia of the Alzheimer type" in the Baltimore Longitudinal Study of Aging. J Clin Epidemiol 1990;43:105–107.
28. National Center for Health Statistics. Vital Statistics of the United States, 1989: Mortality, part A. Washington, DC: Public Health Service; 1993;2:2. [Public Health Service publication 93-1101.]
29. National Institute on Aging/Alzheimer's Association Working Group. Apolipoprotein E genotyping in Alzheimer's disease—consensus statement. Lancet 1996;347:1091–1095.
30. Myers RH, Schaefer EJ, Wilson PWF, et al. Apolipoprotein E ϵ4 association with dementia in a population-based study: the Framingham Study. Neurology 1996;46:673–677.
31. Lee PN. Smoking and Alzheimer's disease: a review of the epidemiological evidence. Neuroepidemiology 1994;13:131–134.
32. Petersen RC, Smith GE, Ivnik RJ, et al. Apolipoprotein E status as a predictor of the development of Alzheimer's disease in memory-impaired individuals. JAMA 1995;273:1274–1278.
33. Hofman A, Bots ML, Breteler MMB, Ott A, Grobee DE. Atherosclerosis and dementia: the Rotterdam Study [abstract]. Neurology 1995;45(suppl 4):A214.
34. The Consortium to Establish a Registry for Alzheimer's Disease (CERAD). Part X. Neuropathology confirmation of the clinical diagnosis of Alzheimer's disease. Neurology 1995;45:461–466.

Quantitative MR volumetry in Alzheimer's disease

Topographic markers and the effects of sex and education

D. Kidron, MD, PhD; S.E. Black, MD, FRCP(C); P. Stanchev, PhD; B. Buck, MSc; J.P. Szalai, PhD; J. Parker, MSc; C. Szekely, MA; and M.J. Bronskill, PhD

Article abstract—We determined topographic selectivity and diagnostic utility of brain atrophy in probable Alzheimer's disease (AD) and correlations with demographic factors such as age, sex, and education. Computerized imaging analysis techniques were applied to MR images in 32 patients with probable AD and 20 age- and sex-matched normal control subjects using tissue segmentation and three-dimensional surface rendering to obtain individualized lobar volumes, corrected for head size by a residualization technique. Group differences emerged in gray and white matter compartments particularly in parietal and temporal lobes. Logistic regression demonstrated that larger parietal and temporal ventricular CSF compartments and smaller temporal gray matter predicted AD group membership with an area under the receiver operating characteristic curve of 0.92. On multiple regression analysis using age, sex, education, duration, and severity of cognitive decline to predict regional atrophy in the AD subjects, sex consistently entered the model for the frontal, temporal, and parietal ventricular compartments. In the parietal region, for example, sex accounted for 27% of the variance in the parietal CSF compartment and years of education accounted for an additional 15%, with women showing less ventricular enlargement and individuals with more years of education showing more ventricular enlargement in this region. Topographic selectivity of atrophic changes can be detected using quantitative volumetry and can differentiate AD from normal aging. Differential effects of sex and years of education can also be detected by these methods. Quantification of tissue volumes in vulnerable regions offers the potential for monitoring longitudinal change in response to treatment.

NEUROLOGY 1997;49:1504–1512

Alzheimer's disease (AD), the leading cause of dementia, presents an increasingly formidable challenge to health care systems as we enter the next century. The need for diagnostic accuracy and for biological and behavioral measures to monitor disease progression and response to therapy has never been more compelling. The present criteria for diagnosis, proposed in 1984,[1] depend heavily on clinical and behavioral analysis. In vivo volumetric and morphometric MR studies can provide sensitive indices of brain anatomy,[2-5] including computer-assisted tissue classification,[6] which in conjunction with appro-

From the Sheba Medical Center (Dr. Kidron), Tel-Aviv, Israel; the Cognitive Neurology Unit, Research Program in Aging (Dr. Black, B. Buck, J. Parker, and C. Szekely), Clinical Epidemiology and Health Care Research Program (Dr. Szalai), and Imaging-Bioengineering Research (Dr. Bronskill), Sunnybrook Health Science Centre, Toronto, Ontario, Canada; and the Institute of Mathematics and Computer Science (Dr. Stanchev), Bulgarian Academy of Sciences, Sophia, Bulgaria.

Supported by grants from the Ontario Mental Health Foundation and the Medical Research Council of Canada. D.K. received fellowship support from Baycrest Centre for Geriatric Care and Sunnybrook Health Science Centre.

Presented in part at the 46th annual meeting of the American Academy of Neurology, Washington, DC, May 1994.

Received March 24, 1997. Accepted in final form June 18, 1997.

Address correspondence and reprint requests to Dr. Sandra E. Black, Head, Division of Neurology, Sunnybrook Health Science Centre, Room A421-2075 Bayview Avenue, North York, Ontario, Canada, M4N 3M5.

Table 1 Demographics and general neuropsychological scores for patients with Alzheimer's disease and normal control subjects

Group	n	Sex	Age (y)	Years of education	Duration of disease (y)	MMSE	DRS total	NART
AD	17	Female	68.3 ± 10.2	12.6 ± 2.4	3.9 ± 2.2	19.5 ± 2.9	109.9 ± 12.2	104.2 ± 10.1
	15	Male	70.6 ± 8.2	12.7 ± 3.6	4.0 ± 2.5	19.1 ± 5.3	102.2 ± 21.4	102.9 ± 9.4
	32	Total	69.4 ± 9.2	12.7 ± 3.0	4.0 ± 2.3	19.3 ± 4.1	106.2 ± 17.4	103.5 ± 9.6
NC	10	Female	74.8 ± 6.7	12.1 ± 1.8	—	28.7 ± 1.0	140.9 ± 2.4	117.8 ± 7.2
	10	Male	72.5 ± 3.9	13.2 ± 2.9	—	27.9 ± 1.1	139.3 ± 2.4	117.8 ± 7.2
	20	Total	73.5 ± 5.4	12.7 ± 2.5	—	28.3 ± 1.1	140.0 ± 3.3	117.1 ± 6.9

Values are means ± SD.

AD = Alzheimer's disease; NC = normal control subjects; MMSE = Mini-Mental State Examination; DRS = Mattis Dementia Rating Scale; NART = New Adult Reading Test.

priate neurobehavioral measures can provide useful tools for the diagnosis and objective documentation of progression in AD and other neurodegenerative diseases.[7-9]

AD is a corticolimbic disease process with definite regional accentuations. Histopathologic studies, as well as functional imaging with PET, have shown that the areas most severely involved are typically the amygdala and hippocampus, temporal and posterior parietal areas, the posterior cingulate gyrus, and the prefrontal lobes.[10-16] Microscopically, the gray matter (GM) is the most affected.[10] Semiautomatic brain tissue segmentation and volumetry methods, including three-dimensional (3D) surface reconstruction, allow investigation of these topographic predilections with anatomical accuracy "customized" for each individual.[16-20] Reliable and accurate structural measurements may also reveal biological effects of demographic factors. For example, advanced age, female sex, and few years of education have been associated with increased incidence of AD.[17-23] The direct relationship of sex and education to brain atrophy, however, has not been adequately investigated.

In this project, we used computerized MRI analysis techniques to determine brain tissue compartment volumes in the major lobar regions of 20 normal elderly subjects (NC) and 32 patients with probable AD. We predicted that the hippocampal formation, parietal, and temporal regions would be most affected by atrophic loss and that the combination of these measurements would be helpful in discriminating AD from control subjects. We used brain tissue segmentation with 3D surface reconstruction to determine, individually in each subject, the volumes of specific lobar regions. The brain variables derived from these procedures were used to investigate topographic selectivity, classification power, and the effects of demographic variables such as age, sex, and education in probable AD.

Methods. *Subjects.* Patients with probable AD were recruited from the Cognitive Neurology Clinic in a large University of Toronto teaching hospital (Sunnybrook Health Science Centre) serving an urban residential community in Toronto, Canada. The group consisted of 32 right-handed community-dwelling patients (15 men and 17 women) who met the National Institute of Neurologic and Communicative Disorders and Stroke and the Alzheimer's Disease and Related Disorders Association diagnostic criteria for probable AD.[1] In addition to the standard tests included in the above criteria, all patients with AD had a modified Hachinski score of 4 or less to reduce the likelihood of vascular dementia.[24,25] The demographic characteristics of all subjects are shown in table 1. Patients with AD had a mean ± SD age of 69.4 ± 9.2 years (range, 50.3 to 84.0). The mean years of education (YOE) was 12.7 ± 3.0 (range, 6 to 18) and the mean duration of disease was 4.0 ± 2.0 years (range, 1.5 to 9.5).

Control subjects were normal volunteers from the community, living at home independently, who were participating in ongoing studies of aging. Subjects with any history of neurologic or psychiatric disease were excluded. The group consisted of 20 right-handed subjects (10 men and 10 women) whose age and education did not differ from the patients with AD. Their mean age was 73.5 ± 5.4 years (range, 67.2 to 88.1) and their mean YOE was 12.7 ± 2.5 (range, 9 to 19).

Patients with AD underwent MRI as part of their clinical workup and received neuropsychological testing on a standardized battery within a mean of 3.3 months of scanning. Similarly, control subjects underwent MRI and received the same neuropsychological protocol within a mean of 0.3 months of scanning. All patients with AD scored below the cutoff level of 123 on the Mattis Dementia Rating Scale[26] and all control subjects scored above. The mean score on the Mini-Mental State Examination (MMSE)[27] for AD patients was 19.5 ± 2.9 (range, 10 to 27) and for control subjects, 28.7 ± 1.0 (range, 26 to 30).

MRI protocol. Brain images were acquired on a 1.5-T Signa system (General Electric Medical Systems, Milwaukee, WI). For the segmentation and lobar volumes, we used a double spin-echo sequence with a 192 × 256 matrix, TR/TE of 3000/30, 80 msec, 0.5 NEX, and a field of view of 20 cm. Imaging time was 11.6 minutes, and 58 3-mm contiguous and interleaved slices were obtained.

Hippocampal measurements were performed on T1-weighted images acquired with a 3D volume technique using a TR/TE of 35/5 msec, 1 NEX, flip angle of 35 degrees, and a field of view of 22 cm. One hundred twenty-four 1.3-mm slices covering the whole brain were acquired in the sagittal plane in an imaging time of 14.4 minutes.

Image analysis. Images were transferred to a Sun SPARC station (Sun Microsystems, Mountain View, CA) for analysis, which involved five major procedures: bifeature segmentation of the whole brain into tissue compartments using proton density and T2-weighted images, ventricular volume calculation, 3D surface reconstruction of the T2-weighted image, lobar definition from 3D surface reconstruction, and hippocampal volume determination from coronal T1-weighted images.

In our pilot study, we carefully investigated different aspects of the acquisition and measurement techniques including the use of filters, correction for nonhomogeneity of the magnetic field, and repeated measurement of the same subject over a short time.[28] We also used different mathematical models for segmentation, brain editing, and 3D reconstruction. The combination of techniques that provided the most reliable results was then selected and used in the current study. High intra- and inter-rater reliability (0.98 and >0.80, respectively) for the bifeature segmentation procedure was established in our pilot study using three raters in 20 subjects.[28]

Bifeature segmentation procedure. Segmentation of the MR images into GM, white matter (WM), and CSF was performed using previously published bifeature segmentation procedures supplied with MRX imaging software by GE Medical Systems.[29,30] Thirty points per compartment (15 per hemisphere) were sampled simultaneously from the proton density and T2-weighted images. The index slice chosen for sampling was the most inferior slice above the level of the orbits where the anterior horns of the lateral ventricles could be seen. WM lesion volumes were not used in the group comparisons because of minimal representation on the index slice. Using a nonparametric statistical algorithm (k-nearest neighbors [KNN] supervised classification), the sampled points were used to derive a "classificator" that determined the most probable tissue type for each voxel.[29,30] The KNN technique was chosen because previous studies have shown that it is the most stable for tissue classification.[31]

Ventricular and sulcal CSF volume calculations. A second procedure was used to semiautomatically define the ventricular CSF (vCSF). A trained observer placed a box around the ventricles in each slice to define the vCSF. Subtraction of the vCSF volume from the total CSF volume yielded by the whole brain segmentation provided a separate estimate of the sulcal CSF (sCSF) volume.

3D surface reconstruction: total brain capacity measurement. A 3D surface rendering technique[32] was used to obtain accurate lobar demarcation using ANALYZE software (version 7.0, Mayo Foundation, Rochester, MN). The T2-weighted image was first "edited" using intensity thresholds and tracing limit lines on each slice to remove nonbrain structures. The whole brain volume, which included brainstem and cerebellum, was then calculated from the edited brain as an index of the total intracranial capacity and was used in the standardization procedures to correct for brain size.

3D surface reconstruction: region of interest definition. Using the edited images, a 3D reconstruction was computed to project the brain surface of each cerebral hemisphere separately. Using anatomical landmarks and a priori geometric rules accepted by neuroanatomic convention, the frontal, parietal, temporal, and occipital lobes were demarcated in the following manner (figure 1).[33] On the lateral surface of each hemisphere, the Sylvian fissure and central sulcus were traced and the parieto-occipital fissure and the preoccipital notch were identified and joined by a line. A line was then drawn from the posterior end of the Sylvian fissure to the line joining the parieto-occipital fissure and preoccipital notch to provide the posterior demarcations of the parietal and temporal lobes. The traced boundaries were projected orthogonally to the medial surface to define lobar-equivalent volumes. The voxels of the lobar region of interest (ROI) were used to mask the segmented images, enabling quantification of the different tissue compartments for each lobe.

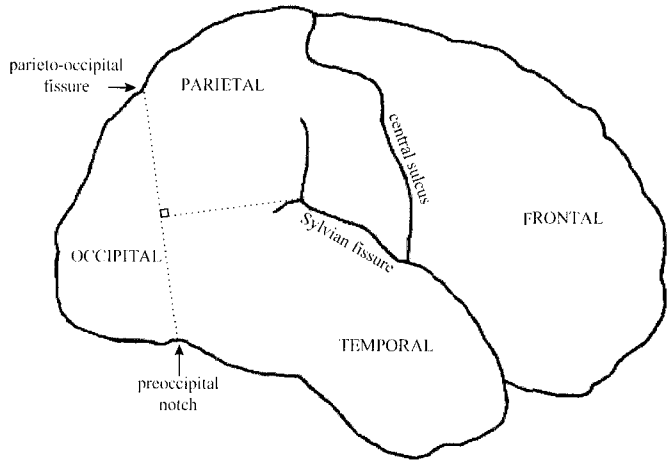

Figure 1. Representational drawing illustrates the location of the sulcal landmarks used in determining lobar volumes.

Hippocampal volume determination. Because tissue compartments could not be discerned in the hippocampus, an automatic procedure could not be applied. To determine the volume of the hippocampus, therefore, a planimetric measurement was obtained. Sagittal images were used to define the anterior and posterior end points of the structure (pes hippocampus and fornix-fimbria, respectively).[34,35] The sagittal images were then reformatted into coronal slices perpendicular to the longitudinal axis of the hippocampal formation. Next, the hippocampal perimeter for each 2.6-mm-thick coronal slice was traced manually for each hemisphere. The demarcated area was multiplied by slice thickness to obtain the hippocampal volume for each slice. The volumes of contiguous hippocampal slices were then summed to provide the total hippocampal volume.

Correction for head size. Several studies established structural volume differences in overall head size between healthy individuals and also between healthy groups of males and females.[36] To correct for normal variation in head size between individuals, a regression model was performed on the total intracranial capacity (as defined previously) in the NC group to yield brain size-residualized volumes, which were then applied to the patients with AD. For the regression model, the intercept was forced to zero based on the assumption that as brain volume approaches zero, the ROI volume should also approach zero. These residualized measures express the ROI volumes as deviations from the predicted volume for an NC with a given intracranial capacity and, by definition, make no assump-

tion of a linear correlation between brain region and total intracranial capacity. In removing the influence of head size from the structural measurements, the regression approach to brain size correction has been shown to be preferable to the use of proportions.[37]

Reliability of measurement techniques. In the present sample, reliability was assessed for the volumetric estimates of GM, WM, and CSF for each ROI. Inter-rater reliability was calculated based on ROI determinations of two independent raters in 18 hemispheres. Intrarater reliability was estimated based on measurements for 10 hemispheres. For the hippocampal volumes, 36 hemispheres were measured for intrarater reliability and 20 for inter-rater reliability. For all regions, the intraclass correlations[38] for intrarater reliability was above 0.82, reaching even higher levels for the vCSF (0.97), temporal lobe (0.94), and hippocampus (0.91). Inter-rater reliability was above 0.70 for all regions.

Statistical methods. The measurements of a single rater (D.K.) were used for all statistical analyses. Five separate MANOVAs (SAS General Linear Models) were performed, one for each region: global, frontal, parietal, temporal, and occipital. Each MANOVA had group (AD or NC) as a between-subjects factor. For each region, the dependent measures included the four tissue compartments (GM, WM, sCSF, and vCSF) in each hemisphere (left and right) except for global region. Any significant multivariate tests were further investigated for univariate effects. Because the hippocampus was not segmentable and only a total volume was derived, a univariate ANOVA was used for this region.

To maintain nominal α at 0.05 for the study, standard top-down statistical procedures were used (proceeding from most general to the most specific comparisons). The significant univariate results from the MANOVAs were further investigated by various statistical procedures, including split-plot ANOVA, logistic regression, and multiple regression, to assess the effects of group, sex, or hemisphere. Forward stepwise logistic regressions designed to predict group membership were performed on both demographic and brain variables. Logistic regression was preferred over discriminant analysis because it has fewer assumptions (e.g., no assumption of multivariate normality for covariates), because it allows categoric and continuous variables to be included, and because it is just as efficient as a discriminant analysis.[39,40] In addition, it also allows the area under the receiver operating characteristic (ROC) curve to be calculated, and this can be useful for diagnosis.

Finally, to explore the effects of demographic factors and disease severity and duration on brain atrophy in AD, the regions that were identified as significantly different between the groups were used as dependent variables in a series of forward stepwise multiple regressions. For each regression, the effects of age, sex, YOE, disease duration, and MMSE as an index of disease severity on regional brain atrophy were examined. To determine the effects of hemisphere, sex, and group, an ANOVA was performed on each of the five dependent variables that differed significantly in the two groups (i.e., frontal vCSF, parietal vCSF, temporal vCSF, temporal GM, and hippocampus as discussed below).

Results. *Group differences in cortical and hippocampal volumes.* Table 2 shows the mean raw volumes of the global and regional GM, WM, sCSF, vCSF, and the hippocampal volumes for the AD and control groups. The percent volume change for each structure is also shown. The MANOVA performed on the residualized global brain volumes with the dependent measures of GM, WM, sCSF, and vCSF revealed a significant multivariate effect of group on the whole brain (Pillai's $F(4,47) = 4.95$, $p = 0.0021$). The MANOVAs performed on residualized left and right GM, WM, sCSF, and vCSF in individual lobes revealed significant multivariate effects of group on frontal (Pillai's $F(8,43) = 2.26$, $p = 0.0413$), parietal (Pillai's $F(8,43) = 2.74$, $p = 0.015$), temporal (Pillai's $F(8,43) = 4.65$, $p = 0.0004$), and occipital (Pillai's $F(8,43) = 2.28$, $p = 0.040$) volumes.

To identify the structural source of the group differences, the univariate effects were further investigated. In the whole brain, there was a significant effect of group on the total GM ($F(1,50) = 7.64$, $p = 0.008$) and total vCSF ($F(1,50) = 14.78$, $p = 0.0003$). For the frontal lobe, there was a significant group effect on left vCSF ($F(1,50) = 14.76$, $p = 0.0003$). The parietal lobe showed significant group effects for both right vCSF ($F(1,50) = 7.68$, $p = 0.0078$) and left vCSF ($F(1,50) = 12.92$, $p = 0.0007$). For the temporal lobe, there were significant group effects on right GM ($F(1,50) = 8.42$, $p = 0.0055$), left GM ($F(1,50) = 12.92$, $p = 0.0007$), right vCSF ($F(1,50) = 9.89$, $p = 0.0028$), and left vCSF ($F(1,50) = 14.91$, $p = 0.0003$). There were no significant univariate effects for the occipital lobe. Note that there were no significant effects on WM and sulcal CSF in any region. For the hippocampus, the univariate ANOVA revealed a group difference ($F(1,44) = 5.36$, $p = 0.0253$) (figure 2).

Group classification. To determine which combination of demographic variables and/or brain tissue volumes could best predict group membership (AD versus NC), forward stepwise logistic regressions were used. Separate models were performed on the demographic variables and then on brain variables to enable assessment of their contribution independent of one another. The demographic variables were age, sex, and YOE, which are known to be risk factors for AD on the basis of epidemiologic studies.[18-20,23] The brain regions were those that significantly differed on the previous MANOVAs. These included the hippocampal, frontal vCSF, parietal vCSF, temporal vCSF, and temporal GM volumes. No demographic factor entered into a prediction equation. Of the available brain variables, however, parietal vCSF, temporal vCSF, and temporal GM entered into and produced a significant model ($\chi^2(3) = 30.81$, $p = 0.0001$). Specifically, larger parietal and temporal vCSF and smaller temporal GM predicted membership in the AD group. The probability that this model correctly distinguished any random pair of individuals, one AD and one NC, in our sample was 0.92 (figure 3, area under the ROC curve).

Demographic markers. To explore the effects of demographic factors on regional brain atrophy in the AD group alone, the regions that were identified as significantly different between groups were used as dependent variables in a series of forward stepwise multiple regressions. This included the frontal vCSF, parietal vCSF, temporal vCSF, temporal GM, and the hippocampus. The independent

Table 2 *Percent volume change of brain structures between patients with Alzheimer's disease and normal control subjects*

Region		Compartment	AD group volume (cm^3)	Control group volume (cm^3)	% volume change*	*p* Value
Global		GM	680.68 ± 101.6	759.40 ± 85.2	−10.4	0.006
		WM	472.00 ± 73.3	476.61 ± 87.3	−1.0	0.838
		sCSF	179.00 ± 53.4	168.67 ± 46.8	+6.1	0.481
		vCSF	50.71 ± 21.4	31.44 ± 15.4	+61.3	0.001
Frontal	R	GM	102.35 ± 20.1	108.72 ± 20.3	−5.9	0.272
		WM	84.48 ± 19.2	89.13 ± 20.2	−5.2	0.409
		sCSF	34.25 ± 17.5	28.20 ± 10.9	+21.4	0.173
		vCSF	8.20 ± 4.2	6.06 ± 5.2	+35.2	0.110
	L	GM	107.46 ± 22.7	114.09 ± 15.2	−5.8	0.253
		WM	91.18 ± 17.7	90.48 ± 25.1	+0.8	0.906
		sCSF	36.34 ± 11.5	35.58 ± 13.3	+2.1	0.828
		vCSF	9.40 ± 4.4	5.53 ± 2.4	+69.9	0.001
Parietal	R	GM	99.01 ± 23.6	105.80 ± 19.4	−6.4	0.282
		WM	58.58 ± 15.3	57.50 ± 12.5	−1.1	0.876
		sCSF	22.68 ± 11.6	21.60 ± 6.3	+19.5	0.270
		vCSF	10.37 ± 7.0	5.20 ± 3.3	+79.5	0.012
	L	GM	99.45 ± 17.6	110.80 ± 19.4	−10.2	0.035
		WM	62.19 ± 15.6	57.50 ± 12.5	+8.1	0.263
		sCSF	23.30 ± 7.7	21.60 ± 6.3	+7.9	0.409
		vCSF	9.32 ± 4.9	5.20 ± 3.3	+79.5	0.002
Temporal	R	GM	78.01 ± 14.1	91.72 ± 15.1	−14.9	0.002
		WM	66.19 ± 15.8	68.96 ± 19.8	−4.0	0.579
		sCSF	22.58 ± 6.7	19.87 ± 6.6	+13.6	0.159
		vCSF	5.52 ± 2.7	3.53 ± 2.0	+56.5	0.006
	L	GM	85.25 ± 12.4	101.51 ± 16.0	−16.0	0.001
		WM	72.76 ± 13.6	69.37 ± 19.8	+4.9	0.466
		sCSF	23.37 ± 5.2	21.60 ± 4.8	+8.1	0.229
		vCSF	7.23 ± 2.81	4.63 ± 2.21	+56.2	0.001
Hippocampus		R	1.09 ± 0.36	1.40 ± 0.34	−20.1	0.011
		L	0.98 ± 0.34	1.25 ± 0.31	−21.2	0.010

Values are means ± SD. Results based on Student's *t*-tests between NC and AD. *Percentages calculated by (AD volume − NC volume)/NC volume.

AD = Alzheimer's disease; GM = gray matter; WM = white matter; R = right; L = left; NC = normal control subjects.

variables included age, sex, YOE, duration of disease, and severity as measured by MMSE.[27] Age, duration, and severity of disease did not significantly contribute to any model. However, breakdown of the variance contributions showed that atrophy as reflected in increased vCSF in the frontal, parietal, and temporal lobes was partially influenced by sex (table 3). For parietal vCSF, for example, sex alone accounted for 27% and YOE accounted for an additional 15% of the variance. Sex also accounted for 16% of the variance for frontal vCSF and for 14% in temporal vCSF. Specifically, female sex was associated with less atrophy (smaller vCSF volumes) and higher education was associated with more atrophy. No effects of these variables emerged for the temporal GM or the hippocampal volumes.

To examine these sex effects in more detail and to compare them with those observed in healthy normal control subjects, four ANOVAs were performed with hemisphere (left, right), sex (male, female), and group (AD, NC) as factors. The dependent measures were the regions that differed significantly in the two groups, namely the frontal vCSF, parietal vCSF, temporal vCSF, and temporal GM. As expected, there was a significant main effect of group in all four brain regions ($p < 0.002$) in that the AD group showed more atrophy (reflected by greater vCSF volume or smaller GM volume) compared with the NC group (figure 4). No group difference interacted with left or right side. A main effect of sex was seen in the temporal GM only, due to smaller volume in males compared with females ($F(1,48) = 5.75$, $p = 0.020$). Significant interactions between group and sex were seen on both the frontal vCSF ($F(1,48) = 5.28$, $p = 0.0260$) and parietal vCSF ($F(1,48) = 7.79$, $p = 0.0075$) (figure 5, a and b). Post-hoc analyses showed that

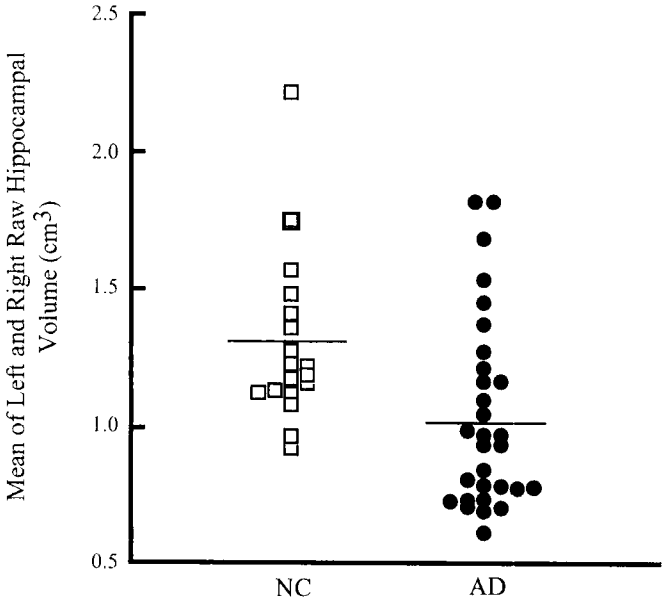

Figure 2. A group difference in the mean of the left and right residualized brain volume was found in the hippocampus, in that AD patients had smaller volumes compare with normal control subjects (NC). To illustrate the overlap in the data, the raw values are plotted here.

in both regions, the AD men had larger vCSF volumes than women, whereas in the NC group, no sex difference occurred. There was no effect of sex or side on the hippocampal volumes.

Discussion. This is the first study in AD as far as we are aware that has used segmentation in combination with surface rendering to measure lobar tissue compartment volumes as defined in each subject individually by conventional surface anatomic landmarks. We also adopted a new technique to correct for brain size that makes no assumptions about linear relationships between brain regions and total head size. Satisfactory inter- and intrarater agreement was achieved, and imaging analysis could be accomplished within 2 hours for each subject. These techniques allowed us to detect sex differences and effects of education on brain atrophy and to capitalize on the known topographic selectivity of AD to distinguish it from normal aging.

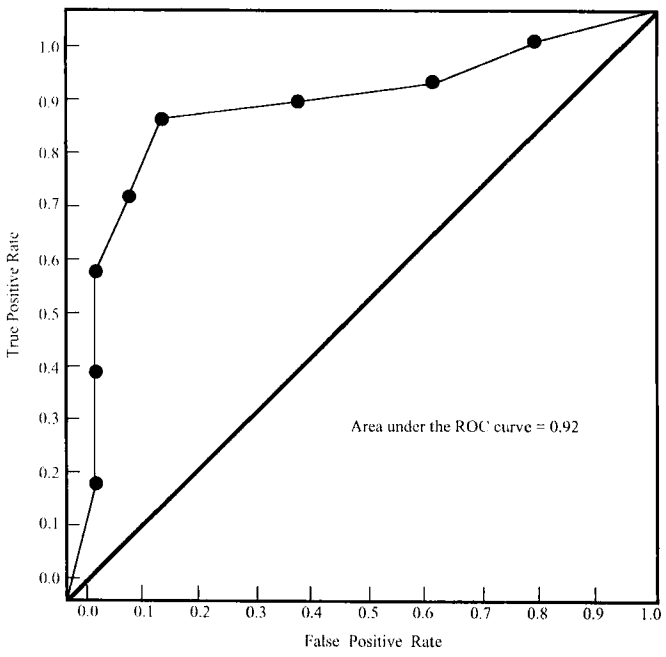

Figure 3. The area under the ROC curve illustrates the high predictability of the model that included temporal GM, temporal vCSF, and parietal vCSF. The probability that this model correctly distinguished any random pair of AD and NC subjects in our sample was 0.92.

Topographic susceptibility in AD. Our results revealed significant differences between the AD and NC groups in certain tissue compartment volumes in selected regions, including the frontal, parietal, and temporal vCSF; temporal GM; and hippocampus, confirming the topographic predilection in AD found by histopathologic[10,11] and other quantitative neuroimaging studies.[41-44]

These results partially concur with one of the first reports of regional volumetry using tissue segmentation in AD subjects.[44] Rusinek et al.[44] used two inversion recovery sequences to sample GM, WM, and CSF compartments and applied standardized region of interest boundaries in a sample of 14 AD and 14 control subjects. They found that regional GM and CSF compartments were strongly correlated, except for the central subcortical region, and that GM and CSF compartments differed significantly in AD subjects both globally and in many regions measured, particularly in the temporal lobe. Our study used a larger sample, customized the region of interest measurements for each individual, and separately evaluated the sulcal and ventricular CSF compartments, the hippocampal formation, and the right and left hemispheres. Our results suggest that the differences in the CSF volumes arise primarily from the ventricular CSF compartment. The fact that temporal GM volume emerged in both studies as significantly reduced in AD subjects, despite differences in techniques of segmentation, regional demarcation, and sample size, suggests that the temporal GM may prove to be a useful discriminator of AD from normal aging. This was supported by logistic regression analysis in our sample.

Although we found a group difference in the hippocampal volumes, there was considerable overlap between AD patients and normal control subjects. Initial MRI volumetric studies suggested that hippocampal atrophy was a promising diagnostic measure of AD.[42] We concur, however, with a subsequent study that suggested hippocampal atrophy alone cannot fully separate patients with AD from NC.[41] Furthermore, it should be noted that hippocampal atrophy may not be restricted to dementia of the AD type.[45]

Classification power. In our study, temporal and parietal atrophy emerged as the best index for correctly identifying patients with AD. The logistic re-

Table 3 *Variance contributions of demographic factors to regional brain atrophy in patients with Alzheimer's disease*

ROI	Demographic variables	β	Partial R^2	Model R^2	F	*p* Value
F vCSF	Sex	3.093	0.162	0.162	5.723	0.023
P vCSF	Sex	5.077	0.265	0.265	10.797	0.003
	YOE	0.666	0.151	0.416	7.505	0.010
T vCSF	Sex	1.560	0.142	0.142	4.945	0.034

Results based on forward regression of residualized scores. Only significant interactions are presented. β denotes direction of slope. Partial R^2 denotes the variance accounted for by each factor alone.

F vCSF = frontal vCSF; P vCSF = parietal vCSF; YOE = years of education; T vCSF = temporal vCSF.

gression, performed to determine which combination of brain variables best predicted group membership, indicated that temporal GM, temporal vCSF, and parietal vCSF best differentiated AD from NC. Our temporal lobe measure included the hippocampus, but because this accounts for less than 1% of total temporal volume, it likely contributes relatively little. Temporal lobe volume emerged as an excellent discriminating variable in early AD in another recent MRI volumetry study.[46] The emergence of temporal and parietal structures as the best predictors of group membership is in keeping with the neocortical topographic selectivity of AD.[10,11]

Important demographic and severity factors. Aging did not affect atrophy in either the AD or NC subjects, possibly because of the relatively narrow age range of our sample. Sex and education, by contrast, emerged as important predictors of atrophy in AD. Epidemiologic studies have consistently shown that women are more likely to develop AD.[47,48] Yet, in terms of tissue loss, our results have indicated that

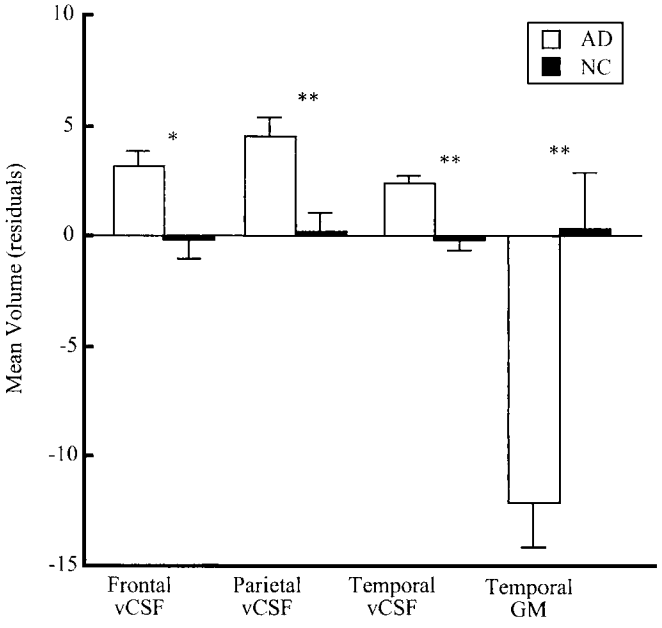

*Figure 4. Group differences in residualized brain volumes were found in four brain regions. Error bars represent the standard error of the mean. *Significant at* $p < 0.003$*; **significant at* $p < 0.0005$.

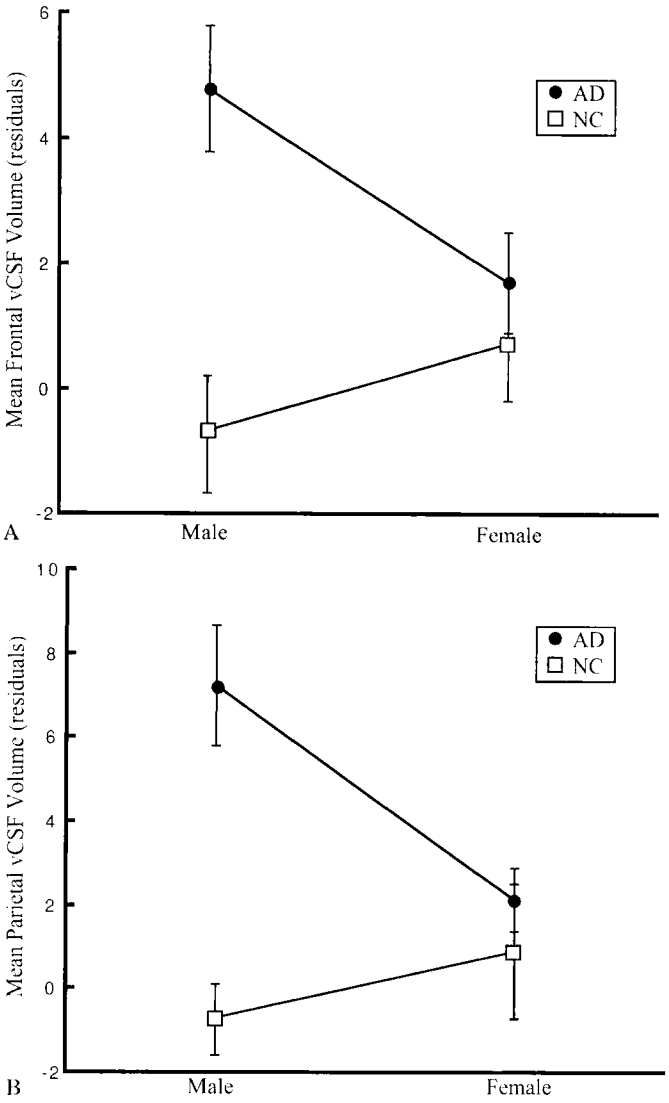

Figure 5. (A) A group by sex interaction was found in the frontal vCSF ($p = 0.0260$*). Post-hoc analyses showed that men with AD had larger vCSF volumes than women with AD (* $p = 0.0226$*), whereas in the NC group, no sex differences were found. (B) Similar results were seen in the parietal vCSF. Upon post-hoc analysis of the group by sex interaction (* $p = 0.0075$*), it was found that men with AD had larger vCSF volumes than women with AD (* $p = 0.0026$*), whereas in the NC group, no sex differences were found. Error bars represent the standard error of the mean.*

women with AD show less brain atrophy (as indexed by CSF volume) than men with AD for the same age, degree, and duration of dementia. Less brain atrophy in normal female subjects has been reported by Gur et al.,[49] although in that study the sex differences were age-related. Our finding of less atrophy in women with AD despite no apparent difference in the other factors, which included severity of cognitive dysfunction, implies that clinical disease expression as indexed by the MMSE is actually more severe in women for the same degree of atrophy. This suggests that an additional factor in women other than structural tissue loss may be correlated to the degree of cognitive impairment. It is not clear whether this factor may relate to lack of activational effects of estrogen in postmenopausal women or some other sex difference, but clearly this warrants further investigation.

In recent years, several studies have suggested that AD is less prevalent in individuals with more years of education and that this is not just an ascertainment bias.[18-20,23,48] A favorite explanation is that more education may protect individuals longer from clinically expressing the disease. This implies that for patients with similar clinical severity of disease, the more educated will be more advanced biologically and show greater AD pathology.[18-20,23,48] There is one functional imaging study that lends support to this concept. In a Xenon inhalation regional cerebral blood flow study in AD subjects matched for cognitive severity, significantly greater parietotemporal hypoperfusion was demonstrated in the more highly educated group, indicating more functional impairment as indexed by blood flow for the same level of cognitive performance.[19] As far as we are aware, our study is the first to show a direct correlation between education and brain tissue volumes. Education may be a surrogate measure for a combination of factors, including inborn intellectual capacity, social-economic status, and degree of lifelong mental stimulation, a neural correlate of which may be synaptic connectivity.[18] Recent pathologic studies suggest that synaptic density is the best correlate of severity of cognitive decline in AD subjects.[50] Zhang et al.[20] and Katzman et al.,[23] among others, have proposed that education may be an index of increased brain reserve, possibly reflecting increased synaptic density in the neocortex. Our study demonstrates a direct relationship between years of education and parietal atrophy and lends further support to the concept that education may have a tardive effect in the clinical evolution of AD.

The outcome of the present study suggests that this method of analysis of the MR images, particularly the segmentation and boundary demarcation, with the additional use of the head size-residualization method, enables an individualized approach to brain measures in AD. A sparse combination of regional volumes can differentiate AD from normal aging. The ability to quantify specific vulnerable regions could allow monitoring of longitudinal change and may help to differentiate AD from other disorders. These possibilities certainly warrant further investigation.

Acknowledgments

We thank J. Foster, M. Moscovitch, and G. Winocur for helping in the pilot study for this project and G. Cheung for assisting in determining hippocampal landmarks. We also thank S. Köhler for his useful comments on the manuscript.

References

1. McKhann G, Drachman D, Folstein M, Katzman R, Price D, Stadlan EM. Clinical diagnosis of Alzheimer's disease: report of the NINCDS-ADRDA Work Group under the auspices of Department of Health and Human Services Task Force on Alzheimer's Disease. Neurology 1984;34:939–944.
2. Filipek PA, Kennedy DN, Caviness VS, Rossnick SL, Spraggins TA, Starewicz PM. Magnetic resonance imaging-based brain morphometry: development and application to normal subjects. Ann Neurol 1989;25:61–67.
3. Jack CR. Brain and cerebrospinal fluid volume: measurement with MR imaging. Radiology 1991;178:22–24.
4. Rademacher J, Galaburda AM, Kennedy DN, Filipek PA, Caviness VS. Human cerebral cortex: localization, parcellation, and morphometry with magnetic resonance imaging. J Cogn Neurosci 1992;4:352–374.
5. Scheltens P, Weinstein HC, Leys D. Neuro-imaging in the diagnosis of Alzheimer's disease. I. Computer tomography and magnetic resonance imaging. Clin Neurol Neurosurg 1992;94: 277–289.
6. Prichard JW, Brass LM. New anatomical and functional imaging methods. Ann Neurol 1992;32:395–400.
7. Golomb J, de Leon MJ, Kluger A, George AE, Tarshish C, Ferris SH. Hippocampal atrophy in normal aging: an association with recent memory impairment. Arch Neurol 1993;50: 967–973.
8. Jernigan TL, Archibald SL, Berhow MT, Sowell ER, Foster DS, Hesselink JR. Cerebral structure on MRI. Part I. Localization of age-related changes. Biol Psychiatry 1991;29:55–67.
9. Jernigan TL, Salmon DP, Butters N, Hesselink JR. Cerebral structure on MRI. Part II. Specific changes in Alzheimer's and Huntington's diseases. Biol Psychiatry 1991;29:68–81.
10. Brun A, Gustafson L. Distribution of cerebral degeneration in Alzheimer's disease: a clinico-pathological study. Arch Psych Neurol Sci 1976;223:15–33.
11. Braak H, Braak E. Neuropathological staging of Alzheimer-related changes. Acta Neuropathol 1991;82:239–259.
12. Foster N, Chase TN, Mansi L, et al. Cortical abnormalities in Alzheimer's disease. Ann Neurol 1984;16:649–654.
13. Haxby JV, Grady CL, Koss E, et al. Longitudinal study of cerebral metabolic asymmetries and associated neuropsychological patterns in early dementia of the Alzheimer type. Arch Neurol 1990;47:753–760.
14. Terry RD, Masliah E, Hansen LA. Structural basis of the cognitive alterations in Alzheimer disease. In: Terry RD, Katzman R, Bick KL, eds. Alzheimer disease. New York: Raven Press, 1994:179–196.
15. West MJ, Coleman PD, Flood DG, Troncoso JC. Differences in the pattern of hippocampal neuronal loss in normal ageing and Alzheimer's disease. Lancet 1994;344:769–772.
16. Friedland RP, Budinger TF, Koss E, Ober BA. Alzheimer's disease: anterior-posterior and lateral hemispheric alterations in cortical glucose utilization. Neurosci Lett 1985;53:235–240.
17. Katzman R, Saitoh T. Advances in Alzheimer's disease. FASEB J 1991;5:278–286.
18. Mortimer JA, Graves AB. Education and other socioeconomic determinants of dementia and Alzheimer's disease. Neurology 1993;43:S39–S44.
19. Stern Y, Gurland B, Tatemichi TK, Tang MX, Wilder D, Mayeux R. Influence of education and occupation on the incidence of Alzheimer's disease. JAMA 1994;271:1004–1010.
20. Zhang M, Katzman R, Salmon D, et al. The prevalence of dementia and Alzheimer's disease in Shanghai, China: impact of age, gender and education. Ann Neurol 1990;27:428–437.
21. Aronson MK, Ooi WL, Morgenstern H, et al. Women, myocar-

dial infarction, and dementia in the very old. Neurology 1990; 40:1102–1106.
22. Hill LR, Klauber MR, Salmon DP, et al. Functional status, education, and the diagnosis of dementia in the Shanghai survey. Neurology 1993;43:138–145.
23. Katzman R. Education and the prevalence of dementia and Alzheimer's disease. Neurology 1993;43:13–20.
24. Hachinski VC, Iliff LD, Zilhka E, et al. Cerebral blood flow in dementia. Arch Neurol 1975;32:632–637.
25. Rosen WG, Terry RD, Fuld PA, Katzman R, Peck A. Pathological verification of ischemic score in differentiation of dementias. Ann Neurol 1980;7:486–488.
26. Mattis S. Mental status examination for organic mental syndrome in the elderly patient. In: Bellak L, Karasu TB, eds. Geriatric psychiatry: a handbook for psychiatrists and primary care physicians. New York: Grune & Stratton, 1976:77–121.
27. Folstein MF, Folstein SE, McHugh PR. "Mini-Mental State": a practical method for grading the cognitive state of patients for the clinician. J Psych Res 1975;12:189–198.
28. Foster J, Black SE, Stanchev P, et al. Regional brain-behavior correlations using magnetic resonance volumetric measures in Alzheimer's disease [abstract]. Ann Neurol 1993;34:293.
29. Cline HE, Lorensen WE, Kikinis R, Jolesz F. Three-dimensional segmentation of MR images of the head using probability and connectivity. J Comp Assist Tomog 1990;14: 1037–1045.
30. Kikinis R, Shenton ME, Gerig G, et al. Routine quantitative analysis of brain and cerebrospinal fluid spaces with MR imaging. J Magn Reson Imag 1992;2:619–629.
31. Clarke LP, Velthuizen RP, Phuphanich S, Schellenberg JD, Arrington JA, Silbiger M. MRI: stability of three supervised segmentation techniques. Magn Reson Imag 1993;11:95–106.
32. Robb RA. Visualization methods for analysis of multimodality images. In: Thatcher RW, Hallett M, Zeffiro T, John ER, Huerta M, eds. functional neuroimaging: technical foundations. San Diego: Academic Press, 1994:181–190.
33. Barr ML, Kiernan JA. The human nervous system: an anatomical viewpoint, 6th ed. Philadelphia: J. B. Lippincott, 1993.
34. Bronen RA, Cheung G. Relationship of hippocampus and amygdala to coronal MRI landmarks. Magn Reson Imag 1991; 9:449–457.
35. Bronen RA, Cheung G. MRI of the normal hippocampus. Magn Reson Imag 1991;9:497–500.
36. Schlaepfer TE, Harris GJ, Tien AY, Peng L, Lee S, Pearlson GD. Structural differences in the cerebral cortex of healthy female and male subjects: a magnetic resonance imaging study. Psych Res Neuroimag 1995;61:129–135.
37. Mathalon DH, Sullivan EV, Rawles JM, Pfefferbaum A. Correction for head size in brain-imaging measurements. Psychiatry Res 1993;50:121–139.
38. Fliess JL. The design and analysis of clinical experiments. New York: John Wiley & Sons, 1986:1.
39. Harrell FE, Lee KL. The practical value of logistic regression. Proceedings of the Tenth Annual SAS Users Group International Conference. Cary, NC: SAS Institute Inc., 1985:1031–1036.
40. Press SJ, Wilson S. Choosing between logistic regression and discriminant analysis. J Am Stat Assoc 1978;73:699–705.
41. Jack CR, Petersen RC, O'Brien PC, Tangalos EG. MR-based hippocampal volumetry in the diagnosis of Alzheimer's disease. Neurology 1992;42:183–188.
42. Kesslak JP, Nalcioglu O, Cotman CW. Quantification of magnetic resonance scans for hippocampal and parahippocampal atrophy in Alzheimer's disease. Neurology 1991;41:51–54.
43. Murphy DGM, DeCarli CD, Daly E, et al. Volumetric magnetic resonance imaging in men with dementia of the Alzheimer type: correlations with disease severity. Biol Psychiatry 1993;34:612–621.
44. Rusinek H, de Leon MJ, George AE, et al. Alzheimer disease: measuring loss of cerebral gray matter with MR imaging. Radiology 1991;178:109–114.
45. Laakso MP, Partanen K, Riekkinen P, et al. Hippocampal volumes in Alzheimer's disease, Parkinson's disease with and without dementia, and in vascular dementia: an MRI study. Neurology 1996;46:678–681.
46. Killiany RJ, Moss MB, Albert MS, Sandor T, Tieman J, Jolesz F. Temporal lobe regions on magnetic resonance imaging identify patients with early Alzheimer's disease. Arch Neurol 1993;50:949–954.
47. Rocca WA, Amaducci LA, Schoenberg BS. Epidemiology of clinically diagnosed Alzheimer's disease. Ann Neurol 1986;19: 415–424.
48. Friedland RP. Epidemiology, education, and the ecology of Alzheimer's disease. Neurology 1993;43:246–249.
49. Gur RC, Mozley PD, Resnick SM, et al. Gender differences in age effect on brain atrophy measured by magnetic resonance imaging. Proc Natl Acad Sci USA 1991;88:2845–2849.
50. Terry RD, Masliah E, Salmon DP, et al. Physical basis of cognitive alterations in Alzheimer's disease: synapse loss is the major correlate of cognitive impairment. Ann Neurol 1991; 30:572–580.

Quantitative MR volumetry in Alzheimer's disease: Topographic markers and the effects of sex and education

D. Kidron, S. E. Black, P. Stanchev, et al.

Neurology 1997;49;1504-1512
DOI 10.1212/WNL.49.6.1504